Exciton Level Structure and Energy Disorder of the B850 Ring of the LH2 Antenna Complex

H.-M. Wu,[†] M. Ratsep,[†] I.-J. Lee,[‡] R. J. Cogdell,[§] and G. J. Small*,[†]

Ames Laboratory—USDOE and Department of Chemistry, Iowa State University, Ames, Iowa 50011, Department of Chemistry, College of Natural Science, Dongguk University, Kyongju City, Kyongpook 780-714, Korea, and Division of Biochemistry and Molecular Biology, Institute of Biomedical and Life Sciences, University of Glasgow, G128 QQ, U.K.

Received: May 5, 1997; In Final Form: July 2, 1997[⊗]

Experimental and theoretical results are presented on the exciton level structure of the B850 ring of bacteriochlorophyll *a* molecules for the light-harvesting 2 (LH2) complex of *Rhodopseudomonas acidophila* (strain 10 050) and the effects of energy disorder (due to structural heterogeneity) on the level structure. The work is an outgrowth of the accompanying paper (Wu et al. *J. Phys. Chem. B* **1997**, *101*, 7641), which reports on the temperature and pressure dependencies of the LH2 absorption spectrum and the zero-phonon hole action spectrum of the lowest energy exciton level of the complex, B870, as well as the structural (nondenaturing) change of the complex near 150 K. The effects of energy disorder are analyzed using the theory of Wu and Small (*Chem. Phys.* **1997**, *218*, 225), which employs symmetry-adapted energy defect patterns. The analysis leads to a room temperature value of ∼100 cm^{-1} for the splitting between B870 and the adjacent, strongly allowed E_1 level in the absence of disorder. Using the temperature-dependent data of Wu et al., we arrive at a theoretical estimate for this splitting at temperatures below ∼150 K of ∼150 cm^{-1}, which is 50 cm^{-1} smaller than the "apparent" value of 200 cm^{-1} based on the 4.2 K B870 action spectrum. The 50 cm^{-1} difference is explained in terms of a distribution of values for the energy disorder parameter(s), which leads to a distribution of values for the oscillator strength of B870. Hole-burning data on the temperature dependence of B870's optical dynamics are presented and analyzed. Below ∼15 K the dynamics are dominated by two-level systems of the protein with an effective dephasing frequency that carries a T^{α} dependence with $\alpha \approx 1.3$. At temperatures above ∼20 K the dephasing is strongly exponentially driven with an activation energy of ∼100−140 cm^{-1}. A mechanism suggested for this dephasing is that it is due to upward scattering of the B870 level to the adjacent E_1 level by one-phonon absorption. New satellite hole spectra for the LH2 complex (isolated and chromatophores) are presented that lead to the assignment of the weak high-energy tail absorption of the B800 and B850 absorption bands to B850 exciton levels of the B850 ring, which are either symmetry forbidden or predicted to be very weakly absorbing in the absence of energy disorder.

1. Introduction

In the accompanying paper[1] (hereafter referred to as I) high-pressure and temperature-dependent absorption and hole-burned spectra for the light-harvesting complex 2 (LH2 or B800−850) of *Rhodopseudomonas acidophila* (strain 10 050) and *Rhodobacter sphaeroides* were presented. (The reader is referred to the Introduction of I for discussion of recent studies of the structures, $Q_y(S_1)$ electronic states, and excitation energy transfer and relaxation dynamics of LH2 complexes.) The primary focus of I was to compare the LH2 complex of *Rps. acidophila*, for which a structure is known,[2] with that of *Rb. sphaeroides* for which a structure is unavailable. The LH2 complex of the former species is a cyclic C_9 array of α,β-polypeptide pairs that bind nine bacteriochlorophyll *a* (BChl *a*) molecules responsible for absorption near 800 nm and nine BChl *a* dimers that absorb near 850 nm (room temperature values). The arrangement of the 18 BChl *a* molecules of the B850 ring is shown in Figure 1 of I. It was concluded that the packing of the α,β pairs for *Rb. sphaeroides* is looser than for *Rps. acidophila*, consistent with weaker excitonic coupling in the B850 ring and a higher value of the compressibility for the LH2 complex of the former species.

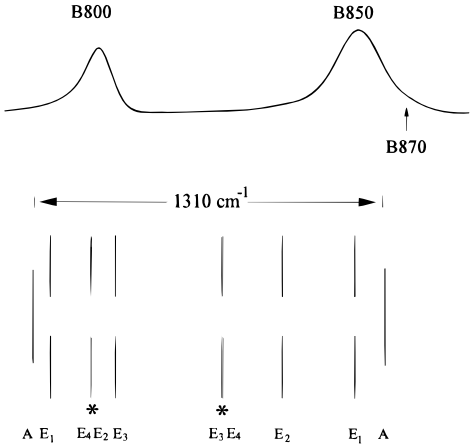

Figure 1. The 4.2 K absorption spectrum of LH2 complex from *Rps. acidophila* (strain 10 050) and exciton manifold of the B850 ring. The manifold was calculated using eqs 1−3 with $e_u - e_l$, V_l, V_u, and V_{ul} equal to 600, −200, 100, and 130 cm^{-1}, respectively. The labels A and E_1−E_4 correspond to the irreducible representations of the C_9 group. The vertical arrow locates B870, the lowest level of the B850 ring (see ref 7). The asterisks indicate two closely spaced doubly degenerate levels.

Of particular relevance to this paper are the following findings reported in I: the LH2 complex of both species in the glycerol/water solvent used undergoes a structural change near 150 K;

[†] Iowa State University.
[‡] Dongguk University.
[§] University of Glasgow.
[⊗] Abstract published in *Advance ACS Abstracts,* August 15, 1997.

S1089-5647(97)01514-9 CCC: $14.00

the nearest neighbor BChl *a*−BChl *a* coupling(s) within the B850 ring is a factor of about 1.4 times stronger for the low-temperature structure; this coupling for *Rb. sphaeroides* is a factor of about 1.2 times weaker than for *Rps. acidophila* at all temperatures; the thermal broadening of the B850 band for both the low- and high-temperature structures is consistent with phonon-assisted relaxation between exciton levels that contribute to the B850 band. The most important contributing levels carry A and E_1 symmetry with the E_1 level responsible for almost all of the absorption intensity of the B850 absorption band.[3,4] The former level is often referred to as B870 and, based on the room temperature X-ray structure for the LH2 complex of *Rps. acidophila*, is predicted to be essentially forbidden in absorption with an intensity substantially less than 1% of the E_1 level.[3] These electronic structure calculations predict that B870 should lie close to 100 cm^{-1} below the E_1 level. In what follows we denote this energy gap by ΔE. An experimental determination of ΔE is an important benchmark for electronic structure calculations.

The only values of ΔE currently available were determined by zero-phonon hole (ZPH) action spectroscopy.[5−7] As discussed in I, the value of ΔE has decreased as the quality of the samples studied has improved. (A perfectly reasonable definition of increasing quality or decreasing structural heterogeneity is a decrease of the B800 and B850 absorption bandwidths at all temperatures.) For example, for samples of *Rb. sphaeroides*, which yielded 4.2 K B850 absorption widths of 280 and 230 cm^{-1}, $\Delta E = 250$ and 185 cm^{-1} at 4.2 K, respectively, while for samples of *Rps. acidophila*, which yielded 4.2 K widths of 430 and 200 cm^{-1}, values for ΔE of 270 and 200 cm^{-1} were reported. In ref 7 it was found that B870 of *Rps. acidophila* carries ∼3% of the intensity of the B850 band, a value that is significantly greater than the predicted value. (For samples exhibiting a 4.2 K B850 bandwidth as narrow as 200 cm^{-1}, B870 is observable as a weak but distinct low-energy feature of the B850 absorption band.[7]) In view of the above results for ΔE it is apparent that the average value of ΔE depends on the extent of structural heterogeneity or, equivalently, the extent of diagonal and off-diagonal energy disorder within and between B850 rings of the ensemble. Recently, Wu and Small[8] introduced symmetry-adapted basis energy defect patterns (BDP) for analysis of energy disorder in cyclic arrays of coupled chromophores. Since any energy defect pattern can be written as a superposition of the orthogonal BDP, determination of the effects of each BDP allows for a systematic approach to the question of whether or not energy disorder can account for spectroscopic data given a zero-order C_n Hamiltonian. The effects include splitting of degenerate exciton levels, modification of interexciton level spacings, and redistribution of oscillator strength. Utilizing the zero-order Hamiltonian of Sauer et al.[3] for *Rps. acidophila*, which yields a ΔE value of ∼100 cm^{-1} in the absence of disorder, Wu and Small found that diagonal and/or off-diagonal energy disorder cannot increase ΔE to the apparent experimental value of 200 cm^{-1} without endowing B870 with far too much absorption intensity, ca. 15% of the intensity of the B850 absorption band.

In this paper we extend the work of Wu and Small by taking into account (i) the result from I that nearest neighbor BChl *a*−BChl *a* coupling(s) of the B850 ring increases by ∼35% below 150 K, at which temperature the structural change occurs, and (ii) a distribution of energy disorder parameter values associated with LH2 complexes of the ensemble. It is shown, for example, that an important consequence of the latter is a strong increase in the transition dipole strength for B870 of an individual LH2 complex as its energy displacement below the E_1 level increases due to energy disorder. As a result, the aforementioned experimental values for ΔE are only *apparent* and need to be corrected for the just-mentioned dependence in order to arrive at a ΔE value for the complex in the absence of energy disorder. Such a value is estimated for both the low- and high-temperature LH2 structures of *Rps. acidophila*. It is the value for the high-temperature structure that is most relevant to electronic structure calculations, since only a room temperature X-ray structure is available. Spectral hole-burning data on the temperature dependence of the spectral dynamics of B870 are reported that provide a reasonable estimate for the value of ΔE at 4.2 K. Satellite hole spectra are presented that we believe speak to the location of other exciton levels of the B850 ring that are either strictly forbidden in absorption or very weakly allowed in the absence of energy disorder (see I for a relevant discussion of weak features in the absorption spectrum of the LH2 complex). The reader is referred to I for a description of the hole-burning apparatus and discussion of other aspects of the experiments.

2. Background on Electronic Structure of LH2 Complexes

Given that the X-ray structures for the LH2 complex of *Rps. acidophila* and *Rs. molischianum* are known, one can calculate its Q_y electronic structure by simply diagonalizing the $m \times m$ Hamiltonian matrix associated with the m BChl *a* molecules of the complex as was done in refs 3 and 4. For LH2 of *Rps. acidophila*, with its C_9 symmetry, $m = 27$ (9 B800 and 18 B850 molecules), while for *Rs. molischianum*, with its C_8 symmetry, $m = 24$ (8 B800 and 16 B850 molecules). The results of refs 3 and 4 show that the effects of the B800 molecules on the excitonic structure of the B850 ring are small. Thus, we ignore the B800−B850 interactions in what follows. That the exciton levels obtained transform like the irreducible representations of the C_n group is more apparent for the B850 ring when one frames the problem in terms of a dimer of the B850 ring.[8,9] As discussed in I, there are two choices for the dimer (see Figure 1 of I). For either dimer the upper (u) level is essentially forbidden in absorption while the lower (l) is strongly allowed. Irrespective of the choice of dimer, the u and l levels spawn exciton manifolds for the C_n ring. (Since this paper is mainly concerned with the LH2 complex of *Rps. acidophila*, n is taken equal to 9 in our calculations.) The projection operator technique of group theory[10,11] allows for generation of the exact eigenfunctions for both manifolds.[8] In the nearest dimer−dimer coupling approximation, which is, of course, less restrictive than the nearest monomer−monomer coupling approximation, the energies of the two exciton manifolds are given by

$$E_l^j = e_l + 2V_l \cos(2\pi j/n) \quad (1)$$

and

$$E_u^j = e_u + 2V_u \cos(2\pi j/n) \quad (2)$$

where e_l and e_u are the energies of the two levels of the dimer, V_l and V_u are, respectively, the nearest neighbor dimer−dimer coupling energies for the lower and upper manifolds, and $j = 0,1, ..., n-1$ with n the number of dimers in the ring. For $n = 9$, the correspondence between j values and irreducible representations is $j = 0$ (A), $j = \{1,8\}$ (E_1), $j = \{2,7\}$ (E_2), $j = \{3,6\}$ (E_3), and $j = \{4,5\}$ (E_4). Following the generation of the u- and l-manifolds, one needs to consider the interactions between their respective exciton levels. The couplings are given by

$$H_{ul}^{j} = 2V_{ul}\cos(2\pi j/n) \quad (3)$$

Because the Hamiltonian is totally symmetric, the coupling is restricted by symmetry to levels of the same j value. The dimer−dimer couplings V_l, V_u, and V_{ul} can be determined using the monomer−monomer coupling energies.[8] The B850 exciton level structure shown in Figure 2 of I was calculated with $e_u - e_l = 600$ cm^{-1}, $V_u = 100$ cm^{-1}, $V_l = -200$ cm^{-1}, and $V_{ul} = 130$ cm^{-1}, slightly rounded off values determined using the monomer−monomer coupling energies of ref 3, which were calculated using the room temperature X-ray structure for LH2 of *Rps. acidophila*. For convenience, the level structure is shown in Figure 1 along with the 4.2 K absorption spectrum of LH2 for *Rps. acidophila*. The lowest energy and strongly absorbing E_1 level is situated to be coincident with the B850 absorption maximum. As mentioned in the Introduction, the nearest neighbor monomer−monomer coupling(s) of the B850 ring appears to be a factor of 1.4 larger for the low-temperature structure. A difficulty is that the relative contributions to this increase from the two monomers of the dimer associated with the basic α,β-polypeptide unit and nearest neighbor monomers belonging to adjacent α,β-polypeptide units are not known. However, our calculations revealed that the lowest energy A(B870) and E_1 levels and, to a lesser extent, the E_2 level are not very sensitive to how the increase in coupling is distributed (results not shown). The just-mentioned insensitivity is a consequence of V_l and V_u of eqs 1 and 2 carrying opposite sign, vide supra, and the coupling between the l- and u-manifolds being restricted to levels of the same j value. Although the energy ordering for the l-manifold is A(B870) < E_1 < E_2 < E_3 < E_4, the ordering for the u-manifold is reversed. As a result, it is the coupling between the E_3 and E_4 levels of the two manifolds that are most affected by V_{ul} (eq 3), since they are most closely spaced.

The top and middle exciton level diagrams for the B850 ring shown in Figure 2 were calculated with $V_l = -270$ and -320 cm^{-1}, respectively, and values of $e_u - e_l$, V_u, and V_{ul} were the same as given above. The value of -270 cm^{-1} for V_l represents a ∼35% increase over the -200 cm^{-1} value used to obtain the level structure shown in Figure 1. Thus, the larger nearest neighbor BChl *a*−BChl *a* couplings for the low-temperature structure, vide supra, has been attributed entirely to V_l. The exciton level structure for $V_l = -320$ cm^{-1} is shown, in part, because of the possibility that the calculations of Sauer et al.,[3] which lead to $V_l \approx -200$ cm^{-1} for the high-temperature structure, may underestimate the strengths of nearest neighbor BChl *a*−BChl *a* couplings of the B850 ring.[12] Finally, the exciton level diagram shown at the bottom of Figure 2 was calculated using only eq 1 with $V_l = -320$ cm^{-1}; i.e., the u-manifold of the basic dimer and interactions of its exciton levels with those of the l-manifold are neglected. Note that the rightmost E_1 levels of the three energy diagrams in Figure 2 are placed at the same energy and should be referred to the E_1 level of Figure 1, which is coincident with the B850 absorption maximum.

Comparison of the lowest energy A(B870), E_1, and E_2 levels for the three manifolds in Figure 2 shows that ΔE and $E_1 - E_2$ gaps are quite similar. Analysis of the eigenvectors for these levels associated with the upper two manifolds revealed that they are similar to those for the lowest manifold in the figure. This is not the case for the E_3 and E_4 levels as would be expected from earlier discussion. However, our main interest is in the B870 and lowest energy E_1 and E_2 levels. In particular, we are interested in the mixing of the B870 and E_1 levels due to energy disorder, which destroys the cyclic symmetry, thereby bringing

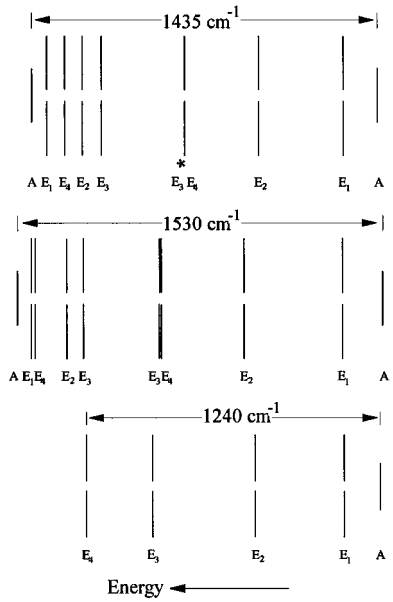

Figure 2. Exciton level manifolds of the B850 ring calculated with different parameter values (the energy scales for the three manifolds are the same). The top and middle manifolds were calculated with $V_l = -270$ and -320 cm^{-1}, respectively, and values of the other parameters are the same as those given in the caption to Figure 1. The bottom diagram shows the l-manifold generated using only eq 1 with $V_l = -320$ cm^{-1} (see text). From top to bottom, the energy gap between B870 and the adjacent strongly allowed E_1 level (ΔE) equals 122, 160, and 150 cm^{-1}, respectively. The asterisk indicates two closely spaced doubly degenerate levels.

absorption intensity to B870 as well as increasing ΔE.[4,8] To this end, it suffices to use the zero-order Hamiltonian for the B850 ring associated with only the l-level of the basic dimer, i.e., the Hamiltonian used to calculate the manifold at the bottom of Figure 2. The essential physics that emerges from our analysis of energy disorder would be unaffected by utilization of the complete Hamiltonian. Also, an exact treatment at this time is unwarranted because it is not clear which of the existing electronic structure calculations for the B850 ring is most reliable.

3. Results and Discussion

In the first part of this section we consider the problem of how energy disorder affects the lower exciton levels of the B850 ring of BChl *a* molecules associated with the B850 absorption band. Although the results of calculations presented are for *Rps. acidophila*, they are relevant to the LH2 complexes of *Rb. sphaeroides* and *Rs. molischianum*. Included also are temperature-dependent hole-burning data for the lowest energy level of the B850 ring, B870, for *Rps. acidophila*, which lead to an estimate for the displacement of this level below the strongly absorbing E_1 level, i.e., ΔE. As mentioned, experimental determination of ΔE is an important benchmark for electronic structure calculations of the exciton level structure of the B850 ring. In the second part, new satellite hole spectra for the LH2 complex of *Rps. acidophila* and *Rb. sphaeroides* are presented that suggest assignment of certain weak features in the Q_y absorption spectrum to other exciton levels of the B850 ring (see I).

A. Energy Disorder and the B850 Ring. In the preceding section it was emphasized that our primary interest is in how energy disorder affects the lowest A(B870), E_1, and E_2 levels of the B850 ring and that the basic physics can be uncovered using a zero-order Hamiltonian, H_0, for the lower, strongly allowed level of the basic dimer of the B850 ring. This

Hamiltonian yields eq 1. In what follows, the subscript l is dropped. We begin with a review of the results of ref 8 where orthogonal basis defect patterns (BDP) were introduced. For C_9, the BDP transform like the $E_{j,\pm}$ irreducible representations with $j = 1-4$. The single nondegenerate BDP is totally symmetric (A). For example, $E_{1,+}$ and $E_{1,-}$ are orthogonal partners for the separably degenerate $j = 1$ and 8 representations of the C_9 group. The Hamiltonian for a C_n array of chromophores (dimers for the case at hand) in the absence of disorder is

$$H_0 = e\sum_{\alpha=0}^{n-1}|\alpha\rangle\langle\alpha| + \sum_{\alpha,\beta=0}^{n-1}{}' V_{\alpha,\beta}|\alpha\rangle\langle\beta| \tag{4}$$

where Greek letters label the dimers or sites and e is the excitation energy of the dimer. The eigenfunctions of H_0 are delocalized and determined by symmetry to be[11]

$$|j\rangle = n^{-1/2}\sum_{\alpha} B^{j\alpha^*}|\alpha\rangle \tag{5}$$

where $B = \exp(i2\pi/n)$. The normalization constant $n^{-1/2}$ holds when overlap between chromophores of the ring is neglected. Since we take the basic unit of the ring to be a dimer, it suffices to make the nearest dimer−dimer coupling approximation, which, with eqs 4 and 5, leads to

$$E_j = e + 2V\cos(2\pi j/n) \tag{6}$$

for the exciton energies with V the nearest neighbor dimer−dimer coupling (V_l of eq 1).

In the presence of disorder the Hamiltonian is

$$H = H_0 + H_\lambda + H_\nu \tag{7}$$

where H_λ governs the diagonal energy disorder of the ring:

$$H_\lambda = \sum_{\alpha}\lambda_\alpha|\alpha\rangle\langle\alpha| \tag{8}$$

H_ν, which defines the off-diagonal disorder, is given by

$$H_\nu = \sum_{\alpha}\nu_\alpha(|\alpha\rangle\langle\alpha+1| + |\alpha+1\rangle\langle\alpha|) \tag{9}$$

For investigation of how these two defect Hamiltonians couple the zero-order delocalized levels it is most convenient[8] to express both in terms of the delocalized wave functions using

$$|\alpha\rangle = n^{-1/2}\sum_{j} B^{j\alpha}|j\rangle \tag{10}$$

Given here are the main results for diagonal energy disorder (H_λ). (The physics revealed by our calculations with H_λ is essentially the same as the physics obtained from H_ν.) For H_λ the coupling between delocalized levels r and s is

$$\langle r|H_\lambda|s\rangle = \frac{1}{n}\sum_{\alpha}\lambda_\alpha B^{(r-s)\alpha} \tag{11}$$

Any chosen energy defect pattern for the ring can be expressed as a superposition of BDP patterns, since they form a complete set.[8] Thus, one can examine the effects of each BDP on the ring exciton structure to determine which, if any, are of primary importance. The projection operator technique of group theory[10,11] can be used to generate the BDP. Incorporation of the BDP in eq 11 leads to[8]

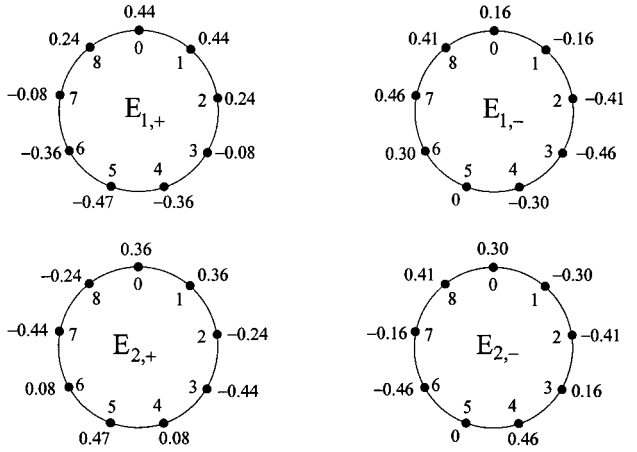

Figure 3. Normalized basis energy defect patterns (BDP) for $E_{1,\pm}$ and $E_{2,\pm}$ of the C_9 group. The numbers inside the circles designate the sites, while those outside the circles are the components of the normalized basis defect vectors (eq 13; see text). The patterns for off-diagonal energy disorder are obtained by rotating the coefficients in the figure by $\pi/9$ to be centered between neighboring dimers.

$$\langle r|H_\lambda^{Ej,\pm}|s\rangle = \frac{\lambda_{j,\pm}N_{j,\pm}}{n}\sum_{\alpha}\left[\cos\left(\frac{2\pi j\alpha}{n}\right) \pm \cos\left(\frac{2\pi j(\alpha-1)}{n}\right)\right]e^{i2\pi\alpha(r-s)/n} \tag{12}$$

for E-type patterns. The + and − signs denote the orthogonal partners of each degenerate pattern. The set of square-bracketed terms obtained with $\alpha = 0,1, ..., n-1$ define the defect pattern. One can define normalized basis defect vectors

$$\boldsymbol{D}_{j,\pm} = N_{j,\pm}(d_{j,0}^{\pm}, d_{j,1}^{\pm}, ..., d_{j,n-1}^{\pm}) \tag{13}$$

where the d-elements are given by the square-bracketed terms in eq 12 and the normalization constant $N_{j,\pm}$ is defined by

$$N_{j,\pm}{}^{-2} = \sum_{\alpha}\left[\cos\left(\frac{2\pi j\alpha}{n}\right) \pm \cos\left(\frac{2\pi j(\alpha-1)}{n}\right)\right]^2 \tag{14}$$

The relationship between $\lambda_{j,\pm}$ in eq 12 and the λ of the generator site defect used with the projection operator technique to obtain eq 12 from eq 11 is $\lambda_{j,\pm}N_{j,\pm}{}^{-1} = \lambda$. Put another way, once the value of the energy defect λ at a particular site (dimer) is defined, the projection operator generates the values of the energy defect at all other dimers. The resulting defect pattern depends on the symmetry of the BDP. The value of $\lambda_{j,\pm}$ is determined by the value of λ and $N_{j,\pm}$. The selection rule associated with eq 12 is

$$r - s = \pm j \tag{15}$$

so that, for example, the $j = \pm 1$ (E_1) diagonal energy disorder pattern couples the $j = 0$ (A) level with the separably degenerate $j = 1$ and $j = n - 1$ (E_1) levels. For n odd, which is the case considered here, the above selection rule also applies to the one and only nondegenerate BDP, $j = 0$ (A) with

$$\langle r|H_\lambda^{A}|r\rangle = \frac{\lambda_0}{n^{1/2}} = \lambda \tag{16}$$

which is independent of r.

Figure 3 shows the diagonal energy disorder patterns for $E_{1,\pm}$ and $E_{2,\pm}$ with the numbers located at the dimer sites defined by the components of $D_{j,\pm}$ (eq 13). The results for all BDP are

TABLE 1: Normalized Coefficients of Basis Defect Patterns for C_9

	site number								
	0	1	2	3	4	5	6	7	8
A	0.333	0.333	0.333	0.333	0.333	0.333	0.333	0.333	0.333
$E_{1,+}$	0.443	0.443	0.236	−0.082	−0.361	−0.471	−0.361	−0.082	0.236
$E_{1,-}$	0.161	−0.161	−0.408	−0.464	−0.303	0	0.303	0.464	0.408
$E_{2,+}$	0.361	0.361	−0.236	−0.443	0.082	0.471	0.082	−0.443	−0.236
$E_{2,-}$	0.303	−0.303	−0.408	0.161	0.464	0	−0.464	−0.161	0.408
$E_{3,+}$	0.236	0.236	−0.471	0.236	0.236	−0.471	0.236	0.236	−0.471
$E_{3,-}$	0.408	−0.408	0	0.408	−0.408	0	0.408	−0.408	0
$E_{4,+}$	0.082	0.082	−0.236	0.361	−0.443	0.471	−0.443	0.361	−0.236
$E_{4,-}$	0.464	−0.464	0.408	−0.303	0.161	0	−0.161	0.303	−0.408

given in Table 1. We note that the BDP from off-diagonal disorder are precisely the same but that in Figure 3 the coefficients of the BDP would be rotated by $\pi/9$ to be centered between neighboring dimers.[8]

Concerning the removal of exciton level degeneracies, it is important to note that the degeneracy of level E_j is removed, in first order, by a BDP with symmetry contained in the symmetric direct product $(E_j \times E_j)_+$. For C_9 and $j = 1-4$, the BDP symmetries are, respectively, E_2, E_4, E_3, and E_1. However, a second-order mechanism for removal of degeneracy exists because of the off-diagonal coupling defined by eq 11 and the associated selection rule (eq 15). These group theoretical predictions are in accordance with the results of calculations presented in ref 8 and below.

The results of ref 8 prove that it is the E_1 components of an energy defect pattern that dominate the mixing of the lowest energy level, B870 (A), of the B850 ring with the adjacent E_1 level (Figure 1). This is expected given the selection rule of eq 15 and that the E_1 level lies closest in energy to B870. Thus, one can use BDP of E_1 symmetry to determine the basic consequences of coupling between B870 and the E_1 level, including the relationship between the energy gap ΔE and absorption intensity of B870. Before the results of our calculations are presented, it is important to point out the connection between the BDP shown in Figure 3 and the Hamiltonian H_λ (eq 8). The values of λ_α are determined by assigning a value of λ_0 to the generator site (dimer), dimer "0", and then calculating the magnitudes and signs of λ_α ($\alpha = 1-8$) using the values of the site coefficients associated with the BDP being considered. As an example, for the $E_{1,+}$ BDP, $\lambda_1 = \lambda_0$ and $\lambda_3 = -0.186\lambda_0$ (Figure 3). Note that the symmetry of each $E_{j,\pm}$ defect pattern dictates that the sign of λ_0 is of no consequence. (However, when considering a superposition of BDP rather than a single BDP, the relative signs of the λ_0 values for different BDP is important;[8] superpositions are not considered in this paper.) It is also the case that the effects of energy disorder on the exciton level structure from $E_{j,+}$ and $E_{j,-}$ patterns are identical for the same value of $\lambda_0 N_{j,\pm}^{-1}$. In what follows we refer to the BDP pattern being used as E_1. Next it is necessary to consider glasslike fluctuations in the value of λ_0 from complex to complex in the ensemble. Gaussian randomness is assumed, and since the sign of λ_0 is irrelevant, a normalized half-Gaussian distribution for λ_0 centered at zero is employed. We show here the results for $V = -320$ cm^{-1} (eq 6) and a width for the half-Gaussian of 140 cm^{-1}. This value for V is appropriate for the low-temperature structure, vide supra. The value for the width is viewed as reasonable given typical values of ∼100−200 cm^{-1} for the inhomogeneous broadening of Q_y transitions in photosynthetic complexes (see I and ref 13 for a discussion of studies related to inhomogeneous broadening).

With $V = -320$ cm^{-1}, the gap (ΔE) between B870 and the E_1 level is 150 cm^{-1} in the absence of energy disorder and B870 is forbidden in absorption. E_1 energy disorder couples the two levels, causing an increase in ΔE and nonzero absorption strength for B870. (B870 can be viewed as stealing oscillator strength from the strongly allowed E_1 level.) The solid rectangles in Figure 4 show how the %-absorption of B870 increases as ΔE increases owing to increasing disorder (λ_0 value). The crosses define the half-Gaussian distribution for λ_0. Multiplying the two curves yields the B870 absorption profile of B870, open circles. The width of 115 cm^{-1} for this profile and its ΔE value of ∼200 cm^{-1} are in good agreement with the low-temperature values determined by ZPH action spectroscopy. Thus, it is clear that the value of ΔE determined experimentally is too large relative to its value in the absence of energy disorder and needs to be corrected for the dependence of B870's oscillator strength on the value of λ_0. By integration of the B870 profile shown in Figure 4, it was determined that B870 carries 7% of the total absorption intensity of the B850 ring, a factor of 2 greater than the experimental value for *Rps. acidophila* reported in ref 7. It was noted in this reference that the stated experimental value of 3% could be too low by ∼2% (due to some uncertainty in the deconvolution analysis). Thus, at this time, we consider the factor of 2 disagreement acceptable.

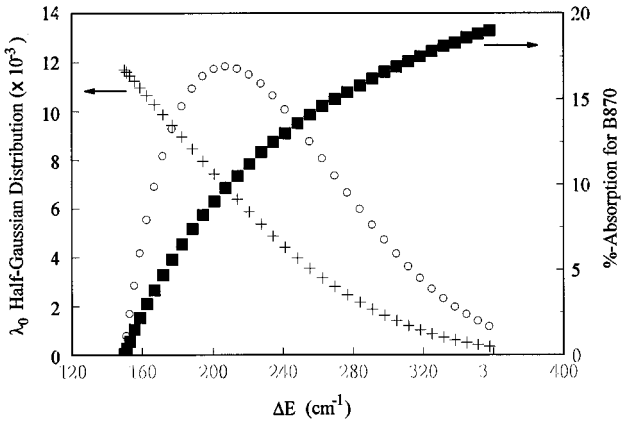

Figure 4. Effect of $E_{1,+}$ diagonal energy disorder on the energy and absorption strength of B870. The solid squares show how the fraction of the B850 ring's total oscillator strength carried by B870 increases with ΔE (the B870−E_1 level energy gap), which increases with increasing disorder (value of the disorder parameter λ_0; see text). The simulated B870 absorption profile is shown by open circles. The crosses define the half-Gaussian distribution for the disorder parameter λ_0. See text for discussion.

The results shown in Figure 4 were obtained using a half-Gaussian distribution for λ_0 with a width of 140 cm^{-1}. It is instructive to examine the exciton level energy diagrams for various values of λ_0. Results are shown in Figure 5 for $\lambda_0 = 0$, 70, 140, and 210 cm^{-1}. The ΔE values are, respectively, 150, 165, 190, and 225 cm^{-1}. (Keep in mind that the probabilities for these λ_0 values are governed by the half-Gaussian distribution.) We note first that the splitting of the highest energy level (E_4) with increasing λ_0 is $0.82\lambda_0$. This is expected, since the

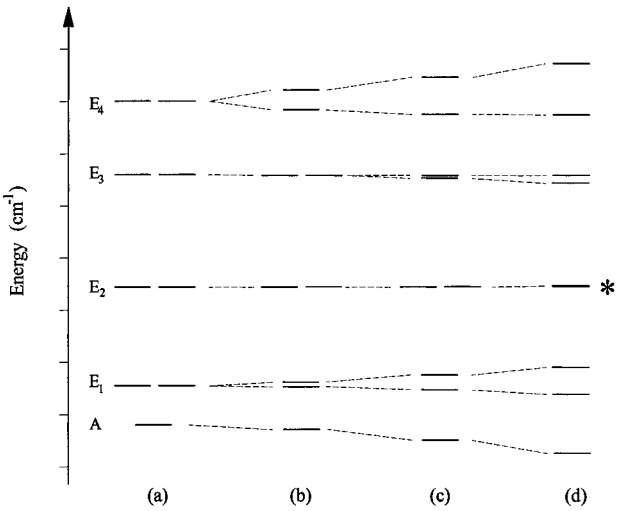

Figure 5. Exciton energy level diagrams for $E_{1,+}$ diagonal energy disorder. From a to d, $\lambda_0 = 0$, 70, 140, and 210 cm^{-1}, respectively. The energy division of the ordinate is 200 cm^{-1}. Dashed lines indicate the correlations of the levels in the presence of disorder with those of the defectless C_9 ring. The asterisk indicates two closely spaced levels. As λ_0 increases, ΔE and the total span of the levels increases. Note the lifting of degeneracies due to disorder. See text for further discussion.

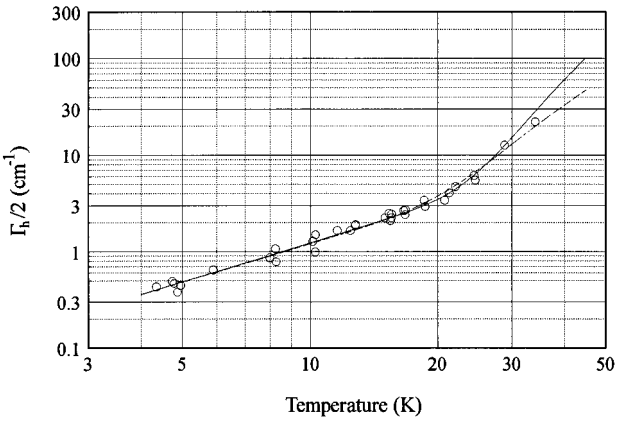

Figure 6. Thermal broadening of B870 ZPH burned in the isolated LH2 complex of *Rps. acidophila* (circles) and two fits calculated using eq 17. ZPH were read with resolutions ranging from 0.5 to 6 cm^{-1}, depending on the temperature region. A resolution of 0.3 cm^{-1} was used periodically to check ZPH burned at about 5 K, and the results were consistent with those shown in the figure. The solid line was obtained with $A = 0.055$ cm^{-1}, $\alpha = 1.35$, $B = 8000$ cm^{-1}, and $\Delta E = 140$ cm^{-1}, while the dashed line was generated with $A = 0.058$ cm^{-1}, $\alpha = 1.31$, $B = 800$ cm^{-1}, $\Delta E = 97$ cm^{-1}.

removal of E_4 degeneracy is, in first order, produced by a BDP of E_1 symmetry, vide supra. As mentioned, a weaker mechanism for removal of degeneracy also occurs because of the energy disorder-induced coupling between different exciton levels, as governed by the selection rule of eq 15. For $\lambda_0 =$ 70, 140, and 210 cm^{-1} the splittings from this higher order mechanism for the E_1 level (due to E_1 energy disorder) are 17, 57, and 103 cm^{-1}, respectively. We give these splittings because the absorption profile of B850 shown in Figure 1 imposes a limit on the extent of energy disorder. This profile is symmetrical in the central region, although a slight bulging appears just to the right (low-energy side) of the B850 maximum. Following the fitting procedure used in ref 7, which takes into account inhomogeneous broadening as defined by the 120 cm^{-1} value for B870 and homogeneous broadening due to interexciton level relaxation, we performed simulations that showed that the splitting of the two comparably intense components of the E_1 levels[8] cannot be much larger than 60 cm^{-1}. (For example, a splitting of 100 cm^{-1} would be apparent in the B850 absorption profile.) It can be seen that the splittings (from the E_1 BDP) given above, when weighted by the λ_0 distribution, lead to a value less than 60 cm^{-1}. Of course, BDP of other symmetries would contribute to the E_1 splitting for an arbitrarily chosen defect pattern.[8] In particular, E_2 BDP (Figure 3) split the E_1 degeneracy in first order by $0.96\lambda_0$ (results not shown). Using the λ_0 distribution defined above with the E_2 BDP yielded an average splitting for the E_1 level of 90 cm^{-1}, somewhat larger than 60 cm^{-1}. Therefore, this λ_0 distribution is reasonably consistent with the low-temperature absorption profile of B850. We hasten to point out, however, that we are considering one BDP at a time and that in the conventional approach of placing Gaussian randomness on the excitation energy at each site of the ring, one would be dealing with superpositions of BDP. Nevertheless, we believe that the λ_0 distribution used provides a useful benchmark for future studies of energy disorder. Furthermore, the level of insight gained by using BDP is unprecedented.

To conclude this subsection, we present the first results on the temperature dependence of the optical dynamics of B870, the lowest exciton level of the B850 ring (Figure 6). The vertical axis corresponds to the zero-phonon hole width of B870 divided by 2, the homogeneous width of the zero-phonon line (ZPL) of B870.[14−16] The data points (circles) for each temperature were obtained by burning and reading at that temperature (shallow holes of fractional depth $\lesssim 0.05$ were used to minimize fluence broadening). The thermal broadening behavior is entirely reminiscent of that observed for the ZPL of isolated molecular chromophores in amorphous hosts such as glasses and polymers[15] with tunneling of the glass two-level systems (TLS) dominating the optical dynamics at lower temperatures and a thermally activated process becoming dominant at higher temperatures. In such systems, however, the latter process usually starts near 10 K and has been ascribed to exchange coupling involving a pseudolocalized phonon of the chromophore, typical frequencies being in the 20−30 cm^{-1} range. (For this mechanism the temperature dependence is governed by the thermal occupation number $\bar{n}(\omega) = [\exp(\hbar\omega/(kT)) - 1]^{-1}$, where ω is the phonon frequency.) Familiarity with this function indicates that the activation energy for the rapid increase in hole width that starts near 20 K in Figure 5 is much higher, ∼100 cm^{-1}. To the best of our knowledge, there is no evidence from hole-burning and photon echo studies for pseudolocalized modes of such high-frequency existing for large chromophores in glasses, polymers, and proteins. It is important to mention the work of Völker and co-workers[17] in which it was reported that the width of ZPH (4.6 cm^{-1}) burned into the B800 band of LH2 is independent of temperature between 1.2 and 30 K. The 4.6 cm^{-1} width is determined by the B800 → B850 energy-transfer process.[17,18] The difference between the temperature dependencies of the B800 and B870 ZPH widths is dramatic, e.g., the B870 hole width at 30 K is 25 cm^{-1}. The rapid increase in B870 dephasing above ∼20 K precluded measurement of its ZPH above ∼35 K owing to the accompanying strong decrease in hole-burning efficiency. In view of the contrasting behaviors of B800 and B870 and that it is very unlikely that a pseudolocalized phonon involving librational type motion of a BChl molecule with a frequency as high as ∼100 cm^{-1} exists, we believe that a different mechanism for the homogeneous broadening that starts near 20 K for B870 is operative. We propose that a significant contribution to this broadening is due to scattering of the B870 exciton level to the adjacent, higher energy E_1 levels due to absorption of bath (protein) phonons with energies equal to the B870−E_1 energy

gap ΔE (energy disorder splits the E_1 degeneracy, vide supra). Such scattering has been thoroughly studied in organic crystals; see, for example, refs 19−21. By necessity, we simplify by using an average value for the energy gaps, ΔE, and express $\Gamma_h/2$ (Figure 5) as

$$\Gamma_h/2 = AT^{\alpha} + B\bar{n}(\Delta E) \qquad (17)$$

where $\bar{n}$ is the previously defined phonon thermal occupation number with phonon energy equal to ΔE. In other words, scattering from the B870 to E_1 level(s) occurs by one-phonon absorption. The first term in this equation is due to the aforementioned TLS of the protein and, possibly, the glass-forming solvent. A multitude of studies on isolated chromophores in amorphous and protein hosts have revealed the universal behavior of $\alpha = 1.3 \pm 0.1$ (see aforementioned references related to TLS). Figure 6 shows two of the fits to the data obtained with eq 17. For the solid and dashed curve fits, $(\Delta E, \alpha) = (140, 1.35)$ and $(97, 1.31)$ cm^{-1}, respectively (the *A* and *B* coefficients are given in the figure caption). All reasonable fits yielded an α value between 1.3 and 1.4. Thus, we are confident that the optical dynamics of B870 at the lowest temperatures is dictated by TLS, although we are unable to determine the contributions to the homogeneous broadening from pure dephasing and spectral diffusion.[15] Particularly interesting is that the magnitude of the TLS-induced homogeneous broadening of B870 is 1−2 orders of magnitude greater than observed for isolated chromophores in amorphous hosts.[14,15,22] Since such a broadening mechanism is relatively unimportant for B800,[17] we plan to investigate, theoretically, whether the strength of this broadening for B870 is a consequence of excitonic delocalization. Our fits to the data of Figure 6 indicate that ΔE lies between ∼100 and 140 cm^{-1}. To reduce this uncertainty would require data for temperatures higher than 35 K as a comparison of the two fits in Figure 5 would indicate. A value of $\Delta E \approx 140$ cm^{-1} based on the optical dynamics of B870 is consistent with our analysis of the ΔE value and the absorption intensity of B870 given above.

To conclude this subsection, we summarize the results that are important for calculations on the electronic structure of the B850 ring of *Rps. acidophila*. For the low-temperature ($T <$ ∼150 K) structure the energy gap (ΔE) between B870 and the allowed E_1 level is close to 150 cm^{-1} in the absence of energy disorder. Inclusion of a physically reasonable amount of energy disorder leads to an apparent value for ΔE of 205 cm^{-1} and B870 carrying ∼7% of the B850 ring's absorption intensity. Based on the results of I, ΔE at room temperature should be close to 100 cm^{-1} in the absence of disorder. This is close to the values calculated by Sauer et al.[3] and Alden et al.[4] The methods employed in these two studies differ in that Alden et al. take into account electron exchange as well as electrostatic interactions and employ a different approach to dielectric screening. We believe the above findings are relevant to the B850 ring of *Rs. molischianum*, since the nearest neighbor distances and orientations of its BChl molecules are nearly identical with those of *Rps. acidophila* and since their B800−B850 energy gaps are nearly the same at all temperatures (the gap for both species being significantly larger than that of *Rb. sphaeroides*[9]). The ZPH action spectrum for B870 of *Rs. molischianum* (isolated LH2 complex) reported in ref 9 led to an apparent ΔE value of 290 cm^{-1}, nearly 100 cm^{-1} larger than the value reported here for *Rps. acidophila*. However, the *Rs. molischianum* samples used in ref 9 yielded a large B850 absorption bandwidth of 355 cm^{-1} at 4.2 K, indicative of significant structural heterogeneity. Given the discussion in the Introduction on the relationship between the apparent ΔE and inhomogeneous spectral broadening, we are confident that the above 290 cm^{-1} value for *Rs. molischianum* would be significantly reduced in LH2 samples exhibiting a B850 absorption bandwidth equal to the 200 cm^{-1} value reported here for *Rps. acidophila*. In future papers on interexciton level relaxation dynamics of the B850 ring (also the LH1 ring) the room temperature and low-temperature (at least 77 K) absorption spectra of the samples studied should be reported so that the extent of structural heterogeneity and energy disorder can be assessed.

B. Satellite Hole Structure Associated with Burning of the B850 Band. The structure being referred to is that of satellite holes that are produced as a result of nonphotochemical hole burning (NPHB) of the B850 absorption band. Under nonline narrowing conditions, the persistent hole produced in the B850 band is broad, as are the satellite holes that lie to higher energy of it, including those that lie within the B800 absorption band. Such satellite hole structure was first reported for the NF 57 mutant of *Rb. sphaeroides* chromatophores[18] (this mutant is devoid of LH1) and, somewhat later, the isolated LH2 complex of *Rps. acidophila*.[6] Because of the weakness of the satellite holes relative to the B850 hole and other factors (see section 4.C of I), they were assigned as intramolecular BChl *a* vibronic features that build, in a Franck−Condon sense, on the B850 "origin" hole. Based on new results, it was argued in section 4.C of I that the vibronic interpretation is most likely incorrect, with proof of this, in the way of new satellite hole spectra, to be presented here. For consideration of the results presented below, we note that a vibronic interpretation of the satellite hole structure requires that the intensities of the satellite holes relative to the B850 hole be essentially invariant to sample preparation, species, or whether the LH2 complex studied is isolated or membrane bound. It will be seen that this is not the case. We emphasize also that all persistent hole-burned spectra of antenna protein complexes reported to date are of the nonphotochemical type and that NPHB is generally observed only for chromophores imbedded in structurally disordered solids such as glasses and polymers or, for example, proteins with their glasslike structural disorder. As a result, the kinetics of NPHB are highly dispersive with a distribution of rates spanning several decades.[23,24] In the current mechanism of NPHB[25] the excess free volume of the glass, which is associated with the TLS,[26] plays a pivotal role.

Figure 7 shows two hole-burned spectra for the isolated LH2 complex of *Rb. sphaeroides* obtained with a burn frequency located on the high-energy side of the B850 band at $\omega_B \approx$ 11 840 cm^{-1}. The burn fluence used to obtain the lower spectrum was a factor of 2 higher than that of the upper spectrum. Features b and b′ correspond to the broad B850 hole mentioned above, and their location relative to the B850 absorption maximum is similar to that reported in ref 18 as is the case for features d, e, and f. These last three features were assigned in that reference to vibronic holes due to ∼340, 750, and 920 cm^{-1} BChl *a* vibrations,[27,28] respectively, which build on the B850 origin band. The problem with the vibronic interpretation is that the intensities of the d, e, and f holes relative to the B850 hole in Figure 6 are significantly higher than those reported in ref 18. For example, the integrated intensity of hole e relative to the B850 hole in the upper spectrum of Figure 7 is 0.5, while in the spectra of ref 18 it is 0.05. (Results presented below for *Rps. acidophila* also negate the vibronic interpretation.) Holes a and a′ in Figure 7 are assigned to B870 as in ref 6. The differences between the hole and antihole (asterisk) structures of the two spectra in the vicinity of B850 are intriguing. For example, the a−b gap in the upper spectrum of

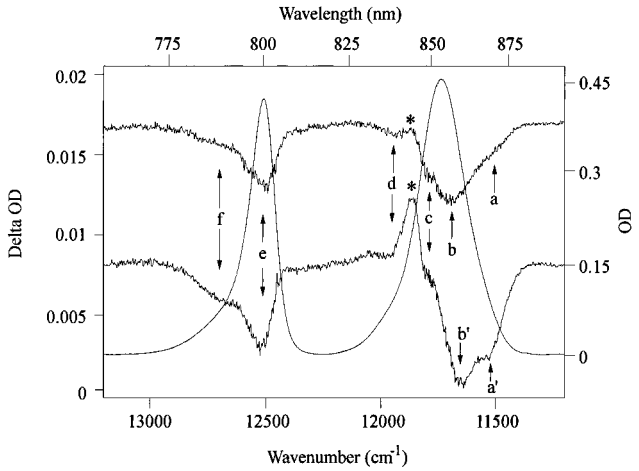

Figure 7. The 4.2 K absorption and hole-burned spectra of LH2 from *Rb. sphaeroides*. The B800 and B850 band maxima (widths) are 12 510 (135) and 11 735 (245) cm^{-1}. The burn frequency is ~11 840 cm^{-1}. The burn fluence employed was 1250 and 2300 J/cm^2 for the upper and lower hole-burned spectrum, respectively. The two hole-burned spectra are offset along the ordinate for clarity.

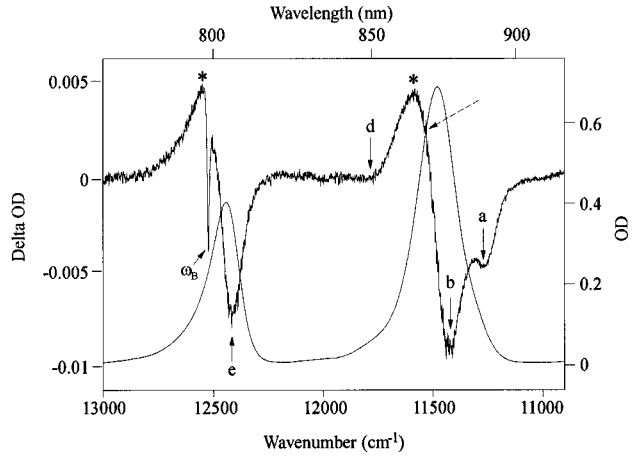

Figure 8. The 4.2 K absorption and hole-burned spectra of LH2 from *Rps. acidophila*. The B800 and B850 band maxima (widths) are 12 440 (160) and 11 475 (220) cm^{-1}. The burn frequency (ω_B) of 12 522 cm^{-1} produced a 4% deep ZPH. The burn fluence employed was 450 J/cm^2. See text for the explanation of the dashed arrow and other details.

Figure 7 is ~200 cm^{-1} while in the lower spectrum it is 120 cm^{-1} (a′−b′). The only interpretation we can offer for the differences is based on the mechanism and dispersive kinetics of NPHB and the results presented earlier in this paper. In the earlier stages of burning (upper spectrum), one tends to burn complexes with B870 levels that are most red-shifted, i.e., complexes with greater energy disorder/structural heterogeneity. That is, there is positive correlation between structural heterogeneity and NPHB efficiency. As one irradiates longer, B870 levels of individual complexes with less structural heterogeneity are burned out. However, understanding the differences between the hole and antihole structures of the two spectra is complicated by the phenomenon of light-induced hole filling (LIHF).[29] LIHF is most efficient when irradiation is in the region of the antihole, which for $\pi\pi^*$ states lies to the blue of the hole (see the antihole (asterisk) in the lower spectrum of Figures 7−9, for example). Since ω_B lies on the blue side of B850, it is likely that some filling of the B850 hole and B870 hole occurs continuously during the burning process and that complexes can undergo multiple burning events. Given this, that NPHB involves a hierarchy of configurational events of the host medium[25] and the hole−antihole interferences, it would

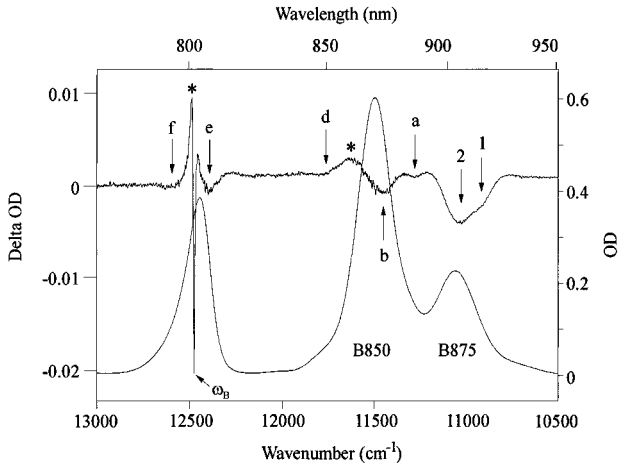

Figure 9. The 4.2 K absorption and hole-burned spectra of *Rps. acidophila* chromatophores. The B800, B850, and B875 band maxima (widths) are 12 445 (150), 11 495 (220), and 11 060 (255) cm^{-1}. The burn frequency (ω_B) of 12 473 cm^{-1} produced a 7% deep ZPH. The burn fluence employed was 225 J/cm^2. See text for other details.

be difficult to achieve a detailed understanding of the evolution of the upper spectrum into the lower spectrum of Figure 7. The inflection feature c was not resolved in the spectra of ref 18 and might correspond to the hole from the higher energy component of the allowed E_1 level split by energy disorder with hole b(b′) being the lower energy component. The antihole of the latter hole interferes with hole c in the same way that the antihole marked by the asterisk interferes with hole d and that of hole e interferes with hole f (see ref 30 for a discussion of such interference). Note that holes d and f coincide with the high-energy tail absorptions of B850 and B800. The question arises as to which exciton level NPHB occurs predominantly in following direct or indirect (B800 → B850 energy transfer) excitation of the B850 band. It is probably the lowest level, B870, since it has a lifetime of several hundred picoseconds, while the E_1 levels possess subpicosecond lifetimes (see I for discussion). NPHB in the B870 exciton level leads to burning of higher energy levels of the B850 ring because they are correlated by excitonic delocalization. This effect was first demonstrated for the BChl *a* antenna complex of *P. aestuarii*.[31]

To further establish that the vibronic assignment for the aforementioned satellite holes is untenable, we present Figures 8 and 9 for the isolated LH2 complex of *Rps. acidophila* and chromatophores used to isolate LH2, respectively (see section 2 of I). By comparison of these figures with Figure 7 for *Rb. sphaeroides*, it is important to note that in Figure 7 the B800−B850 energy gap is 775 cm^{-1} while in Figures 8 and 9 for *Rps. acidophila* the gap is 965 and 950 cm^{-1}, respectively. Although the burn frequencies used to obtain the hole spectra in Figures 8 and 9 are located to the blue of the B800, coincident with the ZPH marked by ω_B, we found, as in refs 6 and 18, that the broad hole and antihole (asterisk) features are similar to those obtained with excitation located within the B850 band (results not shown). In other words, the broad features are mainly due to NPHB following B800 → B850 energy transfer. We ignore, for the moment, holes 1 and 2 in Figure 9 due to the LH1 (B875) complex and compare the LH2 hole spectra in Figures 7−9. First, holes a, b, d, and e appear in all the spectra. Hole f, which is evident in Figures 7 and 9, is not obvious in Figure 8 probably because of its interference with the intense blue-shifted antihole of hole e. Given the ZPH action spectra for B870 reported in I and ref 7 and discussions therein, a firm assignment of hole a to B870 can be made. Hole b is assigned to the components of the strongly allowed E_1 level. As mentioned,

feature c in Figure 7 might be due to the hole of the higher energy E_1 component (the bending over of the antihole of hole b in Figure 8, which is indicated by the dashed arrow, could be due to this component). Hole d coincides with the weak tail absorption on the high-energy side of the B850 band. It is unlikely that this absorption is vibronic (see section 4.C of I for the argument based on intramolecular BChl *a* Franck−Condon factors). Thus, we assign the absorption and hole d to the E_2 level, which is made allowed by energy disorder. The disorder would be expected to split its 2-fold degeneracy and could cause a substantial red shift of the lower energy E_2 component.[8] It was already argued, on the basis of the hole spectra in Figure 7, that the intensity of hole e is far too intense for it to be a vibronic hole building on hole b. The spectra in Figures 8 and 9 for *Rps. acidophila* confirm this. It was also argued, on the basis of Figure 7, that hole f is unlikely to be a vibronic feature building on either B800 or B850 (see also ref 7). Comparison of the B800 absorption profile with the location of hole f indicates that it coincides with the weak absorption tail on the high-energy side of B800.

With the e and f holes unlikely to be vibronic features, the question then is what are they due to. (In Figures 8 and 9, hole e cannot be interpreted as the result of downward energy transfer within the B800 band, since it is produced by irradiation into the B850 band (Figure 7, refs 6 and18, and unpublished results.) Two interpretations (models) are put forth. The first to be considered is suggested by electronic structure calculations,[3,4] which place several of the exciton levels of the B850 ring in the vicinity of the B800 band (see Figure 1). Coupling of these levels to Q_y states of the B800 ring, if sufficiently strong, could then elicit a response of the B800 band to NPHB, which occurs following excitation of levels within the B850 band. The second interpretation is that the protein/BChl *a* structural change produced by the just-mentioned NPHB is not confined to regions in only the vicinity of B850 BChl *a* molecules, i.e., the structural change extends to the B800 ring, thereby producing satellite holes in B800. This model does not require the B800−B850 coupling of the first model. For both models, the extent and nature of the structural heterogeneity could be important, influencing, for example, the intensities of holes e and f relative to the B850 hole b. The experimental results presented here do not allow for distinction between the two models for holes e and f. However, the high-pressure hole-burning and femtosecond pump−probe results for B800 reported in ref 32 strongly indicate that the first model is the correct one for hole f and the high-energy tail absorption of B800 it is associated with. More detailed high-pressure hole-burning studies of the B800 band may lead to assignment of the mechanism responsible for hole e. Such experiments are planned.

Finally, we comment briefly on holes 1 and 2 of the LH1 absorption band (so-called B875) shown in Figure 9. The latter hole is very similar to that observed for B875 of chromatophores of *Rb. sphaeroides*.[5] In that work, however, the B875 band was broader than that of Figure 9 and hole 1 was not resolved. Nevertheless, the lowest energy exciton level of the LH1 ring (see I) with which hole 1 is associated was resolved by ZPH action spectroscopy and found to lie 85 cm^{-1} below the B875 absorption maximum; i.e., the gap analogous to the apparent $\Delta E = 200$ cm^{-1} of B850 is 85 cm^{-1} for B875. From Figure 9, we obtain $\Delta E = 120$ cm^{-1}. Recent theoretical modeling (including energy minimization and molecular dynamics) of the LH1 complex indicates that the orientations of the Q_y transition dipoles of the 32 BChl *a* molecules in the C_{16} ring are similar to those of the B850 ring.[33] Thus, the energy ordering of the B875 exciton levels is expected to be such that the A level (often referred to as B896) lies lowest in energy followed next by the E_1 and E_2 levels, etc. We point out, therefore, that the reduction in the value of the apparent ΔE from 200 cm^{-1} for B850 of *Rps. acidophila* (C_9) to 85 cm^{-1} for B875 is close to the value predicted by eq 6 when it is assumed that the value of V and the energy disorder are similar for the two rings. Equation 6 predicts that ΔE for B875 should be 0.35 times the value for B850. We conclude that the assignment of Reddy et al.[5] of B896 to the lowest energy, weakly allowed exciton level of the LH1 ring is correct.

4. Concluding Remarks

Because of their high cyclic symmetries, the LH1 and LH2 antenna complexes are ideally suited for improving our understanding of excitonic level structure and interexciton level relaxation dynamics in photosynthetic complexes and other nanostructures where strong coupling is important. That the basic α,β-polypeptide pairs of the LH1 and LH2 "rings" are symmetry equivalent simplifies the problem considerably, since the dimers (BChl *a*) of both are energetically equivalent in the absence of glasslike structural heterogeneity of the protein. Such heterogeneity is now known to be important at biological temperatures. However, the effects of energy disorder produced by such heterogeneity on excitonic level structure and dynamics cannot be well understood before the excitonic level structure in the absence of disorder is. Understanding this structure well, even in the absence of disorder, is a nontrivial problem. We have in this work confirmed that B870 is the lowest energy level (A symmetry) of the B850 ring. We further determined values of ∼150 and 100 cm^{-1} for the energy gap (ΔE) between B870 and the strongly allowed and adjacent E_1 level of the B850 ring for the low- and high-temperature structures of *Rps. acidophila*'s LH2 complex, respectively (see I). These values are important benchmarks for electronic structure calculations. The data presented on the temperature dependence of the optical dynamics of the B870 exciton level of *Rps. acidophila* were shown to be consistent with a low-temperature ΔE value in the range of ∼100−140 cm^{-1}. We emphasize again that the structural change of the LH2 complex that occurs near 150 K is by no means anything close to denaturing. The structural change has no effect on the B800 absorption band (see I), but it suffices to alter nearest neighbor BChl *a*−BChl *a* couplings of the B850 ring. (The structural change occurs for both the isolated LH2 complex and the LH2 complex in chromatophores for *Rps. acidophila*, *Rb. sphaeroides*, and *Rs. molischianum* (ref 9 and unpublished results).) Reddy et al. concluded, on the basis of zero-phonon hole action spectra, that B896 is the lowest energy exciton level of the LH1 complex. The results presented here and the structure modeling calculations of ref 8 establish that the assignment for B896 of Reddy et al. is correct.

Additional assignments for the B850 ring's excitonic level structure were made. The weak high-energy tail of the B850 band was ascribed to the lowest energy E_2 level, which borrows intensity from the allowed E_1 level by virtue of energy disorder. The corresponding tail of the B800 band was assigned to the highest energy exciton levels of the B850 ring, which are quasi-resonant with B800. Coupling of these levels with the Q_y states of the B800 ring is one mechanism by which they can attain oscillator strength. As pointed out in refs 1 and 32, such mixing may play a role in the excitation energy relaxation dynamics within the B800 band.

The effects of energy disorder on the level structure of the B850 were examined using the recently introduced symmetry-adapted basis defect patterns (BDP). Only diagonal energy

disorder was considered, since the results obtained with off-diagonal disorder are similar. Attention was focused on the lowest energy A (B870), E_1, and E_2 levels and a BDP of E_1 symmetry, since it couples the A and E_2 levels with the allowed E_1 level. It was shown that there is a strong increase in the transition dipole strength for B870 of an individual LH2 complex as its displacement (ΔE) below the E_1 level increases due to disorder. Thus, the value of ΔE determined by ZPH action spectroscopy (the apparent value) needs to be corrected for this effect. This was done and a value of $\Delta E \approx 150$ cm^{-1}, in the absence of disorder, was obtained for the low-temperature structure. The above results lead to the following picture for the B850 absorption band at low temperatures. Energy disorder removes the degeneracy of the E_1 level with an average splitting of a few tens of cm^{-1} but no greater than $\sim$60 cm^{-1}. For such splittings both components of the E_1 level should carry comparable transition dipole strengths (ref 8 and unpublished results). The disposition of B870 has been discussed. We only add that we were able to reconcile how B870 carries only a few percent of the absorption intensity of the B850 ring when the apparent ΔE value of 200 cm^{-1} is a factor of 2 greater than the calculated values for the room temperature structure. The E_2 level, like B870, borrows intensity from the E_1 level with energy disorder removing its degeneracy. All told, one has five levels that contribute to the overall B850 absorption profile, a finding of relevance, for example, to ultrashort pulse experiments. The above picture should remain essentially intact for the high-temperature structure with some minor differences due to weaker excitonic couplings for the high-temperature structure and, possibly, the structural heterogeneity being temperature dependent. With regard to the latter, it was shown that the effects of energy disorder on the B850 ring's excitonic structure become more important as the inhomogeneous contribution from heterogeneity to the width of the B850 band increases.

Acknowledgment. Research at the Ames Laboratory was supported by the Division of Chemical Sciences, Office of Basic Energy Sciences, U.S. Department of Energy. Ames Laboratory is operated for USDOE by Iowa State University under Contract W-7405-Eng-82. Research at the University of Glasgow was supported by BBSRC and EU. We thank Dr. Klaus Schulten for providing us with preprints of his work prior to publication and for helpful discussions.

References and Notes

(1) Wu, H.-M.; Ratsep, M.; Jankowiak, R.; Cogdell, R. J.; Small, G. J. *J. Phys. Chem. B*, preceding paper.

(2) Freer, A. A.; Prince, S. M.; Sauer, K.; Papiz, M. Z.; Hawthornthwaite-Lawless, A. M.; McDermott, G.; Cogdell, R. J.; Isaacs, N. W. *Structure* **1996**, *4*, 449.

(3) Sauer, K.; Cogdell, R. J.; Prince, S. M.; Freer, A. A.; Isaacs, N. W.; Scheer, H. *Photochem. Photobiol.* **1996**, *64*, 564.

(4) Alden, R. G.; Johnson, E.; Nagarajan, V.; Parson, W. W.; Law, C. J. Cogdell, R. G. *J. Phys. Chem. B* **1997**, *101*, 4667.

(5) Reddy, N. R. S.; Picorel R.; Small, G. J. *J. Phys. Chem.* **1992**, *96*, 6458.

(6) Reddy, N. R. S.; Cogdell, R. J.; Zhao, L. Small, G. J. *Photochem. Photobiol.* **1993**, *57*, 35.

(7) Wu, H.-M.; Reddy, N. R. S.; Small. G. J. *J. Phys. Chem. B* **1997**, *101*, 651.

(8) Wu, H.-M.; Small. G. J. *Chem. Phys.* **1997**, *218*, 225.

(9) Wu, H.-M.; Reddy, N. R. S.; Cogdell, R. J.; Muenke, C.; Michel, H.; Small, G. J. *Mol. Cryst. Liq. Cryst.* **1996**, *291*, 163.

(10) . Tinkham, M. *Group Theory and Quantum Mechanics*; McGraw-Hill: New York, 1964.

(11) Hochstrasser, R. M. *Molecular Aspects of Symmetry*; W. A. Benjamin Inc.: New York, 1966.

(12) Hu, X.; Ritz, T.; Damjanovic, A.; Schulten, K. *J. Phys. Chem. B* **1997**, *101*, 3854.

(13) Jankowiak, R.; Small, G. J. In *Photosynthetic reaction centers*; Deisenhofer, J., Norris, J., Eds.; Academic Press: London, 1993; p 133.

(14) Völker, S. In *Relaxation Processes in Molecular Excited States*; Fünfschilling, J., Ed.; Kluwer Academic Publisher: Dordrecht, 1989; p 113.

(15) Narasimhan, L. R.; Littau, K. A.; Pack, D. W.; Bai, Y. S.; Elschner, A.; Fayer, M. D. *Chem. Rev.* **1990**, *90*, 439.

(16) Jankowiak, R.; Hayes, J. M.; Small, G. J. *Chem. Rev.* **1993**, *93*, 1471.

(17) van der Laan, H.; Schmidt, Th.; Visschers, R. W.; Visscher, K. J; van Grondelle, R.; Volker, S. *Chem. Phys. Lett.* **1990**, *170*, 231.

(18) Reddy, N. R. S.; Small, G. J.; Seibert, M.; Picorel, R. *Chem. Phys. Lett.* **1991**, *181*, 391.

(19) Robinette, S. L.; Stevenson, S. H.; Small, G. J. *J. Chem. Phys.* **1978**, *69*, 5231.

(20) Port, H.; Rund, D.; Small, G. J.; Yakhot, V. *Chem. Phys.* **1979**, *39*, 175.

(21) Robinette, S. L.; Stevenson, S. H.; Small, G. J. *J. Lumin.* **1979**, *18/19*, 219.

(22) Reinot, T.; Kim, W.-H.; Hayes, J. M.; Small, G. J. *J. Chem. Phys.* **1996**, *104*, 793.

(23) Kenny, M.; Jankowiak, R.; Small, G. J. *Chem. Phys.* **1990**, *146*, 47.

(24) Kim, W.-H.; Reinot, T.; Hayes, J. M.; Small, G. J. *J. Phys. Chem.* **1995**, *99*, 7300.

(25) Shu, L.; Small, G. J. *J. Opt. Soc. Am.* **1992**, *B9*, 724.

(26) Cohen, M. H.; Grest, G. S. *Phys. Rev. Lett.* **1980**, *45*, 1271.

(27) Renge, I.; Mauring, K.; Avarmaa, R. *J. Lumin.* **1987**, *37*, 207.

(28) Gillie, J. K.; Small, G. J.; Golbeck, J. H. *J. Phys. Chem.* **1989**, *93*, 1620.

(29) Shu, L.; Small, G. J. *J. Opt. Soc. Am.* **1992**, *B9*, 738.

(30) Lee, I.-J.; Hayes, J. M.; Small, G. J. *J Chem. Phys.* **1989**, *91*, 3413.

(31) Johnson, S. G.; Small, G. J. *J. Phys. Chem.* **1990,** *95*, 471.

(32) Wu, H.-M.; Savikhin, S.; Reddy, N. R. S.; Jankowiak, R.; Cogdell, R. J.; Struve, W. S.; Small, G. J. *J. Phys. Chem.* **1996**, *100*, 12022.

(33) Hu, X.; Schulten, K. Technical Report UIUC-TB-97-02; University of Illinois at Urbana−Champaign, 1997.